# Stabilised aluminium phosphate nanoparticles used as vaccine adjuvant

Vrieling, H.; Espitia Ballestas, M.; Hamzink, M.; Willems, G.J.; Soema, P.; Jiskoot, W.; ... ; Metz, B.

Colloids and Surfaces B: Biointerfaces 181 (2019) 648–656

Contents lists available at ScienceDirect

Colloids and Surfaces B: Biointerfaces

journal homepage: www.elsevier.com/locate/colsurfb

# Stabilised aluminium phosphate nanoparticles used as vaccine adjuvant

Hilde Vrieling[a,b], Margarita Espitia Ballestas[a], Martin Hamzink[a], Geert-Jan Willems[a], Peter Soema[a], Wim Jiskoot[b], Gideon Kersten[a,b], Bernard Metz[a,*]

[a] Intravacc (Institute for Translational Vaccinology), Bilthoven, the Netherlands
[b] Division of BioTherapeutics, Leiden Academic Centre for Drug Research (LACDR), Leiden University, Leiden, the Netherlands

ARTICLE INFO

*Keywords:*
Nanoparticles
aluminium phosphate
Stabilization
Adjuvant
Vaccines

ABSTRACT

Aluminium phosphate is a commonly used adjuvant consisting of heterogeneously sized aggregates up to several micrometers. However, aluminium phosphate nanoparticles may exhibit an improved adjuvant effect. In this study, nanoparticles were made by sonication of commercially available aluminium phosphate adjuvant, resulting in particles with a size (Z-average diameter) between 200–300 nm and a point of zero charge of 4.5. To prevent reaggregation, which occurred within 14 days, a screening of excipients was performed to identify stabilisers effective under physiological conditions (pH 7.4, 290 mOsm). The amino acids threonine, asparagine, and L-alanyl-L-1-aminoethylphosphonic acid (LAPA) stabilised sonicated aluminium phosphate. Particle sizes remained stable between 400–600 nm at 37 °C during 106 days. Contrarily, arginine induced strong reaggregation to a particle size larger than 1000 nm. The stability of aluminium phosphate nanoparticles was strongly affected by the pH. Aggregation mainly occurred below pH 7. The adsorption capacity, a potentially relevant parameter for adjuvants, was slightly reduced in the presence of asparagine, when using a model antigen (lysozyme). LAPA, arginine, threonine and aspartic acid reduced protein adsorption significantly. The adjuvant effect of aluminium phosphate nanoparticles was studied by immunisation of mice with diphtheria toxoid adjuvanted with the aluminium phosphate nanoparticles. The presence of LAPA, threonine, aspartic acid or asparagine did not alter diphtheria toxoid-specific antibody or toxin-neutralising antibody titres. Arginine increased diphtheria toxoid-specific antibody titres but not toxin-neutralising antibody titres. In conclusion, aluminium phosphate nanoparticles were stabilised by particular amino acids and induced an adjuvant effect comparable to that of aluminium phosphate microparticles.

## 1. Introduction

Adjuvants augment the immune response against an antigen. The most commonly used adjuvants for human vaccines are aluminium salts, i.e. aluminium phosphate and aluminium hydroxide [1], [2]. Both adjuvants aggregate to form colloidal particles of a few micrometers in size in water [3], [4]. Aluminium salt-based adjuvants improve the development of immunological memory after vaccination by modulating the uptake [5] and presentation of antigens [6] and by enhancing the humoral immune response [7]. Aluminium salts adsorb antigens mainly via electrostatic interactions or ligand binding [8]. Antigen adsorption influences the stability of the antigen [9], the immune response [9–11] and the cellular uptake and presentation of the antigen [12]. The adsorption degree of vaccine antigens is determined for batch release of vaccines that contain an aluminium salt-based adjuvant. The adsorption capacity is influenced by many factors, such as the charge and size of both the adjuvant and the antigen. Moreover, the surface area of aluminium salt-based adjuvants is very important for protein adsorption [13]. In principle, the surface area increases as the particle size decreases. Besides its effect on antigen adsorption capacity, the particle size of particulate adjuvants is also an important parameter for the immune response. The cellular uptake of particles in general is related to their size and cellular uptake routes differ between small and large particles [14], [15], which may affect the resulting immune responses. For instance, Li et al. reported that the specific antibody responses are stronger and last longer after s.c. immunisation with aluminium hydroxide nanoparticles compared to immunisation with aluminium hydroxide micro particles, and relate these effects to increased antigen adsorption and increased uptake of the adjuvant-antigen complex by APCs when using nanoparticles compared to micro particles [16].

Because the size of a particle may be important for its adjuvant effect, nanoparticles may be beneficial over micro particles as vaccine adjuvant. For instance, it may be possible to decrease the adjuvant dose,

* Corresponding author at: Intravacc, Antonie van Leeuwenhoeklaan 9, 3721 MA Bilthoven, the Netherlands.
*E-mail address:* bernard.metz@intravacc.nl (B. Metz).

https://doi.org/10.1016/j.colsurfb.2019.06.024
Received 20 February 2019; Received in revised form 31 May 2019; Accepted 11 June 2019
Available online 12 June 2019

leading to a reduction in the side effects of aluminium salt-based adjuvants, such as local irritation and inflammation [16]. However, aggregation of nanoparticles is sometimes difficult to overcome. Several factors influence particle aggregation, such as the presence of salts and the pH of the dispersion [17], [18]. Stabilisers can be used to prevent aggregation, for example, by electrostatic or steric stabilisation. For instance, stabilisers may increase the absolute value of the zeta potential of the particles [19], which in turn improves their colloidal stability. An increased zeta potential may also enhance antigen adsorption. However, the use of a stabiliser might have a negative impact on the immune response.

The aim of the current study was to produce stable aluminium phosphate nanoparticles that can be used as vaccine adjuvant. To this end, nanoparticles were prepared by sonication of commercially available aluminium phosphate adjuvant. The aluminium phosphate nanoparticles were stabilised under physiological conditions, i.e. 290 mOsm and pH 7.4, by using particular amino acids. Subsequently, the mechanism of stabilisation was studied and the influence of sonication and the presence of stabilisers on the adsorption degree of a model antigen, lysozyme, was investigated. In addition, an immunisation study in mice showed that diphtheria toxoid adjuvanted with stabilised aluminium phosphate nanoparticles or commercially available adjuvant showed similarly high diphtheria toxoid-specific antibody responses.

## 2. Materials and methods

### 2.1. Chemicals

Aluminium phosphate (Adju-Phos 2%, batches 7224, 9073, 9129, 9297, 9394) was purchased from Brenntag Biosector. The amino acids L-alanine, L-arginine hydrochloride, L-asparagine, L-aspartic acid, L-glutamic acid, L-glutamine, glycine, L-histidine hydrochloride, L-isoleucine, L-leucine, L-lysine hydrochloride, L-methionine, L-phenylalanine, L-proline, L-serine, L-threonine, trans-4-hydroxy-L-proline, L-valine, L-alanyl-L-1-aminoethylphosphonic acid (LAPA) and sucrose were purchased from Sigma-Aldrich. Lysozyme was obtained from Sigma-Aldrich. Diphtheria toxoid (DIF04-44, 4500 Lf/mL in 0.9% (w/v) NaCl) was produced in house.

### 2.2. Preparation of aluminium phosphate nanoparticles

Nanoparticles of aluminium phosphate were prepared by sonication of commercially available aluminium phosphate. Sonication was performed by using a sonifier with a 3-mm tapered microtip coupled to a ½" disrupter horn (Sonifier™ S-450, Branson Ultrasonics, Emerson). Volumes of 10 mL undiluted aluminium phosphate were sonicated while cooling on ice for the time indicated with a pulse ratio on/off of 1 s/2 s at an intensity of 385 W. To prevent sample contamination as a result of tip erosion, a new tip was used for each sonication. Particle size was measured immediately after each sonication using dynamic light scattering (DLS) as described. Only batches with a Z-average diameter smaller than 400 nm were used. Sonicated aluminium phosphate was used immediately after size measurements.

### 2.3. Stability study of sonicated aluminium phosphate nanoparticles

To study the stability of sonicated aluminium phosphate, one volume of 200 mM amino acid solution in ultrapure water was mixed with two volumes of sonicated aluminium phosphate dispersion containing 1.7 mg/mL $Al^{3+}$ ions. The pH was adjusted to 7.4 by using 1 M of sodium hydroxide (NaOH) or 1 M of hydrochloric acid (HCl). To prevent bacterial contamination, samples were prepared aseptically by using a biohazard cabinet, cleaning utensils with alcohol and using sterile starting materials. The osmolality was measured by using an osmometer (Osmomat 3000, Gonotec GmbH). The osmolality was adjusted to 290 mOsm by adding an appropriate volume of 700 mM sucrose solution that was previously adjusted with 1 M of NaOH or 1 M of HCl to pH 7.4. The volume was adjusted to four volumes with ultrapure water. Samples were incubated at 37 °C for a maximum of 106 days.

### 2.4. Determination of particle size

The size (Z-average diameter) of sonicated aluminium phosphate particles was measured by DLS on a Zetasizer Nano ZS (Malvern Instruments Ltd.). Aliquots of 60 µL of each sample containing 10 µg/mL $Al^{3+}$ ions diluted in ultrapure water was measured in single-use polystyrene UV micro cuvettes (BRAND®) at 25 °C. The Dispersion Technology Software (version 7.11) was used for collection and analysis of the data. Each sample was measured in triplicate with an automatic attenuator. The number of runs and the measurement duration were automatically optimised by the software.

### 2.5. Determination of zeta potential

The zeta potential of sonicated aluminium phosphate particles was measured by using a Zetasizer Nano ZS (Malvern Instruments Ltd.). Folded capillary cells (DTS1070, Malvern Instruments Ltd.) were filled with sample containing 0.85 mg/mL $Al^{3+}$ at 25 °C. The Dispersion Technology Software (version 7.11) was used for collection and analysis of the data. Zeta potential values were calculated according to the Smochulowski equation. Each sample was measured in quadruplicate with an automatic attenuator. The number of runs and the measurement duration were automatically optimised by the software.

### 2.6. Adsorption of amino acids to aluminium phosphate

The binding of amino acids to sonicated aluminium phosphate particles was studied by quantification of free amino acid in a mixture containing 1.7 mg/mL $Al^{3+}$ ions of aluminium phosphate nanoparticles and 100 µM amino acid. After overnight incubation at room temperature, the samples were centrifuged at 16,000*g* for 15 min. The amount of free amino acid in the supernatants was determined by reversed phase high-performance liquid chromatography (RP-HPLC). The free amino acid molecules were derivatised with ortho-phthalaldehyde/9-fluorenyl methyl chloroformate and quantified with fluorescence detection. An internal standard containing 0.05 M norvaline and 0.05 M sarcosine was added to correct for the loss of sample during the experiment. Chromatographic analysis was performed on an RP-HPLC system equipped with a Zorbax Eclipse Plus C18 column (2.1 x 150 mm 3.5 µm, Agilent Technologies), Zorbax Eclipse Plus C18 guard (2.1 x 12.5 mm 5 µm Agilent Technologies), column oven (Hewlett Packard), pump (Hewlett Packard), auto sampler (Hewlett Packard), degasser (Hewlett Packard) and fluorescence detector (Agilent Technologies). Mobile phases used were 10 nm $Na_2HPO_4$, 10 mM $Na_2B_4O_7$ pH 8.2 and 5 nM $NaN_3$ (solvent A) and methanol: acetonitrile: water at a ratio of 45:45:10 (v:v:v) (solvent B). The gradient was initiated with 5% solvent B at a flow of 0.420 mL/min. The flow was maintained and the sample was eluted by a linear gradient from 5 to 55% solvent B in 21 min. Subsequently, the column was flushed for 4 min with 100% solvent B with a flow rate of 0.600 mL/min and then equilibrated to the initial conditions. The Agilent OpenLAB Chromatography Data System (CDS) ChemStation Edition Version C.01.06 75 (Agilent Technologies) software was used for data acquisition and mathematical calculations. The adsorption of amino acids to aluminium phosphate was calculated by subtracting the amount of free amino acid in the supernatant from the amount of amino acid that was added.

### 2.7. Adsorption degree of lysozyme to aluminium phosphate nanoparticles in the presence of amino acids

The amount of lysozyme adsorbed to aluminium phosphate

nanoparticles in the presence of amino acids was determined. Therefore, NHS-Fluorescein (5/6-carboxyfluorescein succinimidyl ester, ThermoFisher) was coupled to lysozyme by mixing in a molar ratio of 2:1. The mixture was allowed to react at room temperature while rotating for two hours. Free fluorescein was removed by using disposable PD-10 desalting columns (GE Healthcare). The purified, labelled protein was used to determine the influence of amino acids on the adsorption of lysozyme to aluminium phosphate. Solutions with different amounts of protein were mixed with aluminium phosphate dispersions. The final $Al^{3+}$ concentration was 0.85 mg/mL and the protein concentration ranged from 0 to 4.5 mg/mL. Samples were incubated for one hour at room temperature in a rotary mixer. The samples were centrifuged at 16,000*g* for 15 min. Supernatants were added to a black, V-bottom 96-wells plate (Greiner Bio-One) in a two-fold dilution (100 µL/well). The amount of lysozyme in the supernatants and added protein concentrations was detected by fluorescence at an excitation of 494 nm and emission of 518 nm by using a SynergyMx reader (BioTek). The amount of lysozyme that was present in the samples was calculated with Gen5 software (version 2.09). To calculate the percentage of protein adsorbed on aluminium phosphate, the fluorescence of the supernatant was subtracted from the fluorescence of the amount of protein that was present initially.

### 2.8. Vaccine preparation

Seven formulations were made to study the adaptive immune response in vivo. Each formulation contained 1.7 mg/mL $Al^{3+}$ aluminium phosphate microparticles or aluminium phosphate nanoparticles in combination with 100 mM stabiliser as adjuvant and 10 µg/mL (3 Lf/mL) diphtheria toxoid as antigen. The pH was set to pH 7.4 by using 0.1 and 0.01 M NaOH and HCl. The osmolality was adjusted to 290 mOsm by adding an appropriate volume of 700 mM sucrose solution.

### 2.9. Adsorption degree of diphtheria toxoid

The amount of diphtheria toxoid that was adsorbed to aluminium phosphate in the vaccines was determined by using an enzyme-linked immuno sorbent assay (ELISA). A volume of 1.5 mL of each vaccine formulation was centrifuged at 13,000*g* for 15 min. Supernatants were analysed for diphtheria toxoid content. To this end, ELISA plates (clear flat-bottom high binding microplates, Greiner Bio-One) were coated overnight at room temperature with 100 µL/well of 0.6 AU/mL horse anti-diphtheria (produced in house) in 0.04 M sodium carbonate, pH 9.6. Plates were incubated with two-fold serial dilutions (100 µL/well) of the supernatants in phosphate buffered saline, pH 7.2, containing 1.06 mM $KH_2PO_4$, 155 mM NaCl, 2.97 mM $Na_2HPO_4$ (PBS, Gibco, Thermo Fisher Scientific) with 0.05% (v/v) polysorbate 80 at 37 °C for two hours. On each plate, the original toxoid DIF04-44 was used to set up a calibration curve with a range of 0.002–0.3 Lf/mL. Plates were washed with 0.05% (v/v) polysorbate 80 in distilled water and incubated with 100 µL/well of horse anti-diphtheria toxoid conjugated to horseradish peroxidase (produced in house) which was 3,000x diluted in PBS supplemented with 0.05% (v/v) polysorbate 80 and 0.5% (w/v) Protifar (Nutricia) at 37 °C for 1.5 h. Plates were washed twice with 0.05% (v/v) polysorbate 80 in distilled water and incubated with 100 µL/well peroxidase substrate (Sure Blue TMB Microwell Peroxidase Substrate, SeraCare Life Sciences) at room temperature for ten minutes. The reaction was stopped by addition of 100 µL/well 0.2 M $H_2SO_4$ (Sigma). The absorbance was read at 450 nm with a plate reader (Bio-Tek reader EL808). Toxoid concentrations were calculated with GraphPad Prism version 7.01. To calculate the adsorption degree of diphtheria toxoid to aluminium phosphate nanoparticles, the amount diphtheria toxoid that was present in each supernatant was subtracted from the amount of diphtheria toxoid that was added.

### 2.10. Immunisation study

The animal experiment was in agreement with the Animal Research: Reporting of in vivo Experiments guidelines and was approved by an independent ethical committee (the animal experiments committee (DEC) of the National Institute for Public Health and the Environment (RIVM)) and the central committee animal studies (The Hague, the Netherlands), following the procedures of the European legislation guideline (2010/63/EU) and the Dutch law for animal testing (WOD).

Specific pathogen-free BALB/c mice (Charles River), 8 weeks old, were divided in groups of 10 animals which consisted of five males and five females and housed per gender and per group. All mice received a single dose containing 0.85 mg $Al^{3+}$, 1.5 Lf DIF04-44 and 50 µmol amino acid in a total volume of 500 µL via subcutaneous injection in the left groin on day 0 and 21. Animals were sacrificed on day 35. Blood was collected in blood collection tubes (MiniCollect 0.8 ml Z Serum Sep GOLD, Greiner Bio-One), and serum was obtained and stored at −20 °C after centrifugation (ten minutes, 3000*g*).

### 2.11. Diphtheria toxoid specific IgG ELISA

Diphtheria toxoid-specific immunoglobulin G (IgG) titres in mouse sera were determined by an ELISA. ELISA plates were coated overnight at room temperature with 100 µL/well of 0.5 Lf/mL diphtheria toxoid in 0.04 M sodium carbonate, pH 9.6. Plates were washed with 0.05% (v/v) polysorbate 80 (Merck) in distilled water and blocked with 1% (w/v) BSA (Serva) in PBS at 37 °C for one hour. Plates were washed with 0.05% (v/v) polysorbate 80 in distilled water and incubated with 100 µL/well two-fold serial dilutions of individual sera in PBS with 0.05% (v/v) polysorbate 80 in ultrapure water at 37 °C for two hours. On each plate, the monoclonal antibody DIM-9 (made in house) was added as a reference. Plates were washed with 0.05% (v/v) polysorbate 80 in distilled water and incubated with 100 µL/well of goat anti-mouse IgG (Southern Biotech) which was 4,000x diluted in PBS supplemented with 0.05% (v/v) polysorbate 80 and 0.5% Protifar (Nutricia) at 37 °C for 1.5 h. Plates were washed twice with 0.05% (v/v) polysorbate 80 in distilled water and incubated with 100 µL/well peroxidase substrate (Sure Blue TMB Microwell Peroxidase Substrate, SeraCare Life Sciences) at room temperature for ten minutes. The reaction was stopped by addition of 100 µL/well 0.2 M $H_2SO_4$ (Sigma). The absorbance was read at 450 nm with a plate reader (Bio-Tek reader EL808). Antibody titres were expressed as the $\log_{10}$ of the serum dilution giving 50% of the maximum optical density at 450 nm for each individual curve and normalised to the titre of aluminium phosphate nanoparticles using GraphPad Prism version 7.01.

### 2.12. Toxin neutralisation test

The diphtheria toxin neutralising capacity of the mouse sera was determined by using a toxin neutralisation test. Sera were inactivated by heating at 56 °C for 45 min and stored at −20 °C. Individual sera were diluted two-fold in complete culture medium (Minimum Essential Media 199 with Hanks' salts and L-glutamine, without sodium bicarbonate (Sigma Aldrich) supplemented with 1 g/L glucose (Gibco, Thermo Fisher Scientific), 1.6 mM glutamine, 1.7 g/L sodium bicarbonate (Gibco, Thermo Fisher Scientific), 5% foetal bovine serum (Serana) and 100 U/mL penicillin and streptomycin (Gibco, Thermo Fisher Scientific)) in 96-well culture plates. Next, 50 µL/well 0.001 Lf/mL diphtheria toxin (Dt125, produced in house) diluted in complete culture medium was added and plates were incubated at 37 °C and 5% $CO_2$ for two hours. Then, 50 µL suspension of Vero cells were added so that each well contained 12,500 cells. Plates were incubated at 37 °C and 5% $CO_2$ for six days. Cell viability was determined using an MTT-based cell proliferation kit (Roche) according to the manufacturer's instructions. Neutralising antibody titres were expressed as the $\log_2$ of the first serum dilution giving 80% of the maximum optical density at 570 nm for each

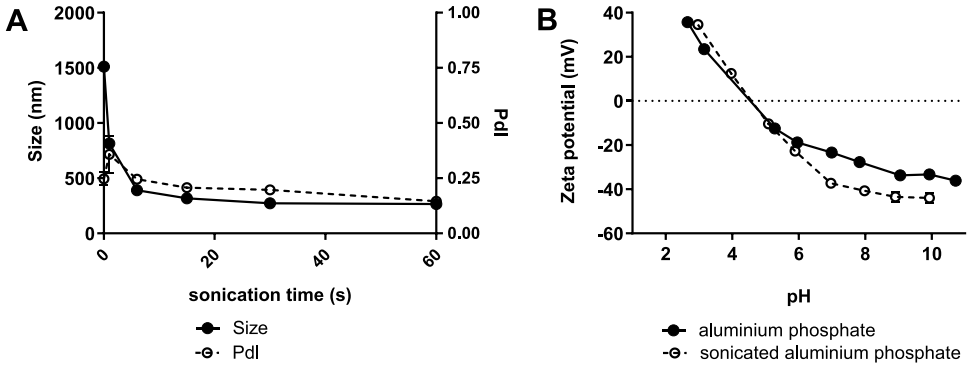


**Fig. 1. Particle size (A) and zeta potential (B) of aluminium phosphate before and after sonication.** (A) Aluminium phosphate was sonicated at 70% of the maximum power output, and at different duration. (B) Aluminium phosphate was sonicated at an intensity of 70% for 60 s. Data is presented as mean ± SD (n = 3).

individual curve.

## 3. Results

### 3.1. Physicochemical properties of aluminium phosphate nanoparticles

The original size of aluminium phosphate was 1455 ± 145 nm with a polydispersity index (PdI) of 0.229 ± 0.036 (Fig. 1A). Sonication for 60 s at 10% or 50% intensity resulted in a reduced size of 404 ± 2 nm or 324 ± 1 nm, respectively (Fig. S1). Sonication at 70%, which was the maximum intensity for the specific tip used, resulted in a fast reduction in size with the biggest reduction taking place during the first 15 s (Fig. 1A). After 60 s, the size of aluminium phosphate was reduced to 273 ± 8 nm. The corresponding PdI was 0.197 ± 0.011, indicating that the particle population was relatively monodisperse. Therefore, in following experiments, sonication was performed at an intensity of 70%. The PdI increased within the first 20 s of sonication. This indicates the generation of particles with different sizes as a result of sonication. After this increase, the PdI decreased, indicating a more homogenous size distribution. Although longer sonication may result in smaller particles, this also enhances tip erosion, introducing contamination from the tip material being present in the sonicated dispersion. Therefore, the maximum sonication time was set at 60 s.

In addition to the size, the point of zero charge (PZC) of aluminium phosphate was determined. Sonication did not change the PZC, which was approximately 4.5 before and after sonication (Fig. 1B). In subsequent experiments, a pH of 7.4 was used to mimic physiological pH.

### 3.2. Stabilisation of aluminium phosphate nanoparticles

To investigate the colloidal stability of aluminium phosphate nanoparticles, the size was monitored for 15 weeks under physiological conditions, i.e. pH 7.4, 290 mOsm (Fig. 2). Within 24 h after sonication, the size increased by a factor of two (215%) compared to the size directly after sonication: from 284 ± 9 nm to 718 ± 10 nm. Between days 1 and 106 the size of sonicated aluminium phosphate still increased, albeit not as fast as in the first 24 h. The size was increased to 895 nm after 106 days. PdI values of all samples with sizes below 1000 nm were between 0.1 and 0.2 (Fig. S4), indicating relatively monodisperse size populations.

To improve the stability of nanoparticles, 26 compounds that are known for their interaction with and/or stabilising effects of colloids, i.e. amino acids, detergents, buffers, sugar alcohols and surfactants, were studied for their stabilising properties. Screening experiments (Table S 1, Fig. S2, Table S2 and Fig. S3) showed that amino acids affected the aggregation of sonicated aluminium phosphate particles the most. For example, the presence of histidine resulted in a size of 620 ± 9 nm, while the presence of glutamic acid induced aggregation of aluminium phosphate nanoparticles resulting in particles with a size of 1102 ± 40 nm. Therefore, an extensive study was performed to investigate the effects of amino acids on the particle size of sonicated aluminium phosphate. The buffering capacity of aluminium phosphate was used to keep the pH at 7.4.

After 106 days incubation, the size of aluminium phosphate in the presence of threonine and LAPA, 465 ± 2 nm and 434 ± 5 nm, respectively, was slightly smaller than that of aluminium phosphate nanoparticles in absence of amino acids (Fig. 2, Fig. S4). The nanoparticles increased the most in the presence of arginine (1462 ± 91 nm), aspartic acid (1049 ± 29 nm) and glutamic acid (1429 ± 243 nm), indicating destabilisation by these amino acids.

The presence of excipients in a suspension may alter the zeta potential of sonicated aluminium phosphate, leading to decreased or increased aggregation propensity of the particles. Therefore, the zeta potential of aluminium phosphate nanoparticles was measured in the presence of the amino acids (Fig. 2). The zeta potential of non-stabilised aluminium phosphate nanoparticles was −13.2 ± 2.4 mV. Most amino acids had limited effect on the zeta potential of the nanoparticles. However, in the presence of lysine the zeta potential became more negative, i.e. −27.8 ± 3.4 mV, which is a notably more negative potential than observed with the other amino acids. The zeta potential of sonicated aluminium phosphate approached −8 mV in the presence of arginine and histidine.

Alterations in zeta potential did not always correlate to the altered size. For example, the presence of arginine resulted in particles with a zeta-potential of −7 ± 1 mV and a size of 1462 ± 91 nm. The presence of histidine resulted in particles with a comparable zeta potential of −9 ± 1 mV. However, the corresponding size of the particles was 839 ± 23 nm. Hence, the effects on the stability could not only be explained by an altered zeta potential compared to the zeta potential of aluminium phosphate without amino acid.

### 3.3. In-depth study of stabilisation by particular amino acids

#### 3.3.1. Influence of pH

The effects of arginine, asparagine, aspartic acid, threonine and LAPA on the stability of aluminium phosphate nanoparticles were further investigated at different pH values. The size and zeta potential of the nanoparticles were monitored between pH 5 and 9 for one week. The pH of the dispersion largely affected the size and zeta potential. For example, the size of aluminium phosphate nanoparticles in the absence of a stabiliser was smaller at pH 8.7 compared to the size at pH 5.7 on day 1, 1491 ± 36 nm and 270 ± 2.4 nm, respectively. The corresponding zeta potential gradually changed from −10.8 ± 1.6 nm at pH 5.7 to −30.3 ± 0.5 nm at pH 8.7 on day 1 (Fig. 3). A similar pattern was observed on day 7, indicating stability for at least one week. The size of sonicated aluminium phosphate was not influenced by asparagine, aspartic acid, threonine and LAPA. However, the size of aluminium phosphate nanoparticles was increased in the presence of

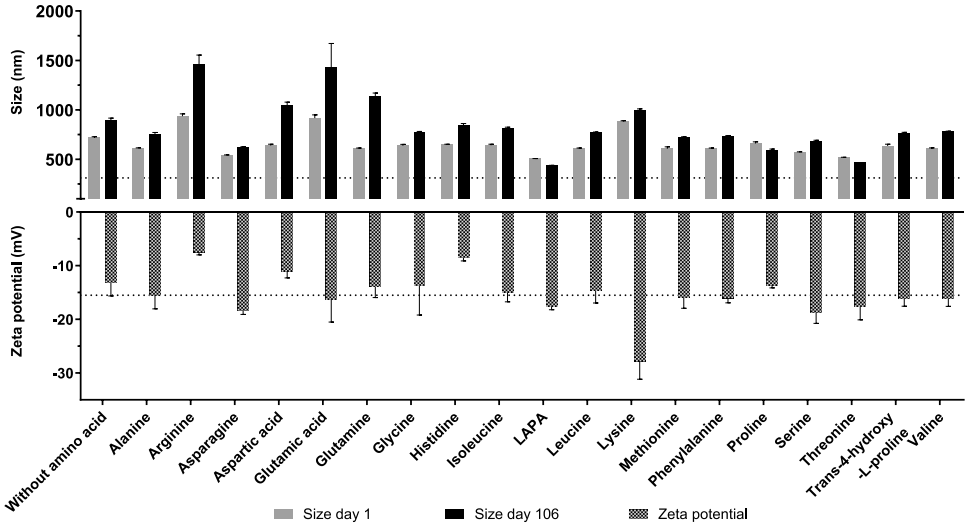


**Fig. 2. Size and zeta potential of sonicated aluminium phosphate in the presence of amino acids.** Sonicated aluminium phosphate was incubated at 37 °C in the presence of 50 mM amino acid. The size was measured weekly with DLS. Here, only the results obtained at day 1 and day 106 are shown. All measurements and PdI values can be found in Supplemental Figure S 4. Dotted lines represent the size and zeta potential of aluminium phosphate nanoparticles immediately after sonication, 311 ± 4.1 nm and −16 ± 2.6 mV, respectively. Data is presented as mean ± SD (n = 3).

arginine irrespective of the pH, varying from 1504 ± 140 nm at pH 5.3 to 636 ± 14 nm at pH 8.0 on day 1. The corresponding zeta potential was −4 ± 1 mV at pH 5.3 and −11 ± 3 mV at pH 8.0 in the presence of arginine. The zeta potential was −7 ± 1 mV at pH 5.4 and −29 ± 2 mV at pH 8.9 in the presence of LAPA. Asparagine, aspartic acid and threonine did not alter the size and zeta potential of the nanoparticles. Although the zeta potential aluminium phosphate nanoparticles in the presence of LAPA was less negative compared to without amino acid, no effects on size were detected. The zeta potential was less negative in the presence of arginine, resulting in an increased size. After one week, the effects of arginine, asparagine, aspartic acid, threonine and LAPA on the size and zeta potential of aluminium phosphate nanoparticles were not different compared to day 1. Thus, the effects of the selected amino acids on the stability of aluminium phosphate nanoparticles were largely affected by the pH of the solution. Only arginine induced aggregation, which can be correlated to the less negative zeta potential values.

### 3.3.2. *Binding of amino acids to aluminium phosphate*

Particular amino acids affect the stability of the aluminium phosphate nanoparticles, resulting in stabilisation or aggregation. The binding of arginine, asparagine, aspartic acid, threonine and LAPA to sonicated aluminium phosphate was investigated by measuring the proportion of amino acid that was adsorbed to the sonicated aluminium phosphate particles by RP-HPLC. Adsorption ranged from 7.0 ± 1.9 nmol/mg $Al^{3+}$ for arginine to 17.8 ± 1.0 nmol/mg $Al^{3+}$ for threonine (Fig. 4). Threonine adsorbed with a significantly higher amount to aluminium phosphate than asparagine, arginine and LAPA. Arginine adsorbed significantly less to aluminium phosphate nanoparticles than aspartic acid, asparagine, threonine and LAPA. No significant differences were found between adsorption of aspartic acid, asparagine and LAPA to aluminium phosphate.

### 3.4. *Effect of amino acid addition on protein adsorption*

The adsorption capacity and adsorption strength are considered

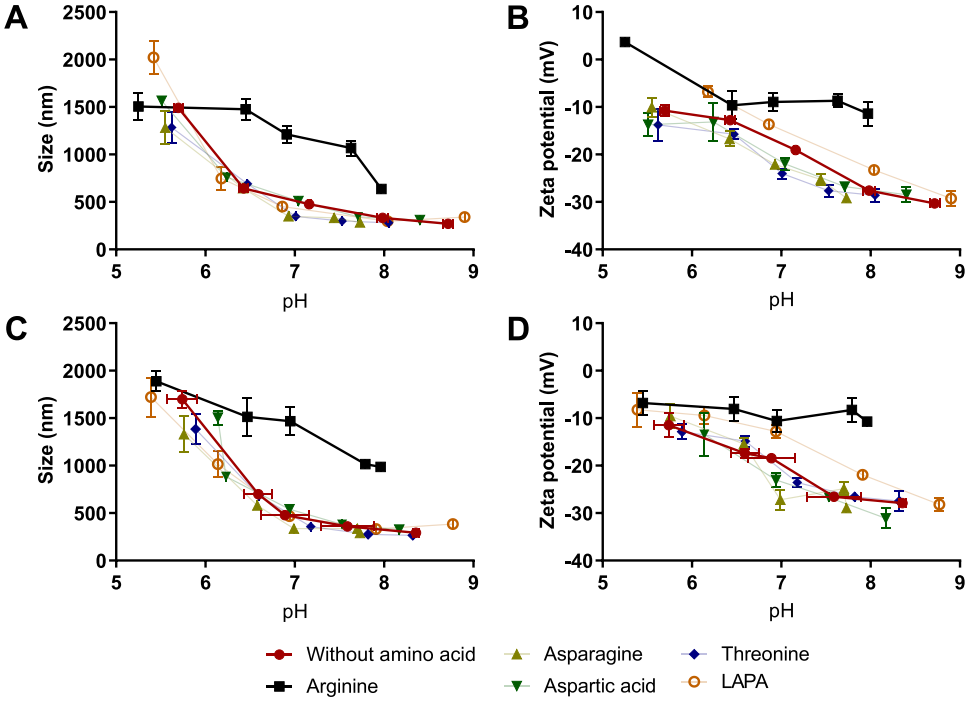


**Fig. 3. pH-stability of sonicated aluminium phosphate in the absence or presence of amino acids at pH 5–9 on day 1 (A and B) and day 7 (C and D).** Size: panels A and C; zeta potential: panels B and D. Sonicated aluminium phosphate was incubated at 37 °C in the presence of 50 mM arginine, asparagine, aspartic acid, threonine or LAPA for 7 days. Data is presented as mean ± SD (n = 3).

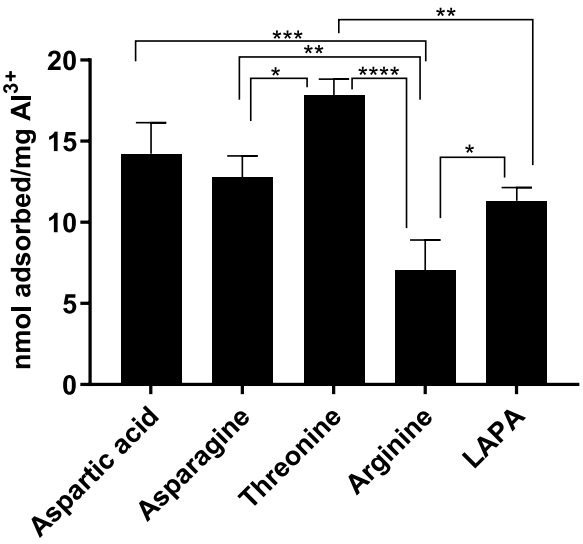


**Fig. 4. Interactions between amino acids and aluminium phosphate nanoparticles.** Sonicated aluminium phosphate containing 1.7 mg/mL $Al^{3+}$ ions was mixed with 100 μM amino acid. Samples were incubated overnight and centrifuged at 16,000 g. The adsorption of amino acids to aluminium phosphate was determined by subtracting the amount of free amino acid in the supernatant from the amount of amino acid that was added. Data is presented as mean ± SD (n = 3). P-values were determined by one-way ANOVA with Tukey's multiple comparison test (* = $p < 0.05$, ** = $p < 0.01$, *** = $p < 0.001$, **** = $p < 0.0001$).

important factors for the initiation of an immune response after vaccination [5]. The adsorption capacity of aluminium phosphate nanoparticles was studied by using the model protein lysozyme. The IEP of lysozyme is 11.35 [20]. At physiological pH, aluminium phosphate and lysozyme are oppositely charged, forming optimal adsorption circumstances. The adsorption capacity was 1.6 ± 0.2 mg lysozyme/mg $Al^{3+}$ ions for sonicated aluminium phosphate in the absence of a stabiliser. This was not significantly higher than that of the original aluminium phosphate (1.3 ± 0.3 mg lysozyme/mg $Al^{3+}$) (Fig. S5).

Addition of amino acids reduced the adsorption of lysozyme to aluminium phosphate nanoparticles (Fig. 5). The highest adsorption degree of the stabilised aluminium phosphate nanoparticles was measured in the presence of asparagine. The adsorption degree of lysozyme to aluminium phosphate nanoparticles decreased even more in the presence of LAPA, threonine, arginine and aspartic acid.

### *3.5. Effect of amino acid addition to aluminium phosphate on the adaptive immune response against diphtheria toxoid*

The immunogenicity of diphtheria toxoid in combination with aluminium phosphate nanoparticles in the presence of amino acids was tested in vivo. Therefore, mice were injected twice with an experimental diphtheria toxoid vaccine containing aluminium phosphate nanoparticles in combination with either aspartic acid, asparagine, threonine, arginine or LAPA. The size and zeta potential of the vaccines as well as the adsorption degree of diphtheria toxoid were determined. Aluminium phosphate nanoparticles aggregated to particles with a size larger than 4000 nm in the presence of arginine, while the size of aluminium phosphate nanoparticles remained below 800 nm in the presence of asparagine, LAPA, threonine or aspartic acid (Fig. 6A). The zeta potential of aluminium phosphate nanoparticles was negative in the presence or absence of amino acids (Fig. 6A). Arginine reduced the zeta potential from −38 ± 1.4 mV to −11 ± 5.5 mV. The adsorption degree of diphtheria toxoid to aluminium phosphate varied from 83% to 96% of the added amount of antigen (Fig. 6B). The amino acids did not influence the adsorption degree significantly compared to that of

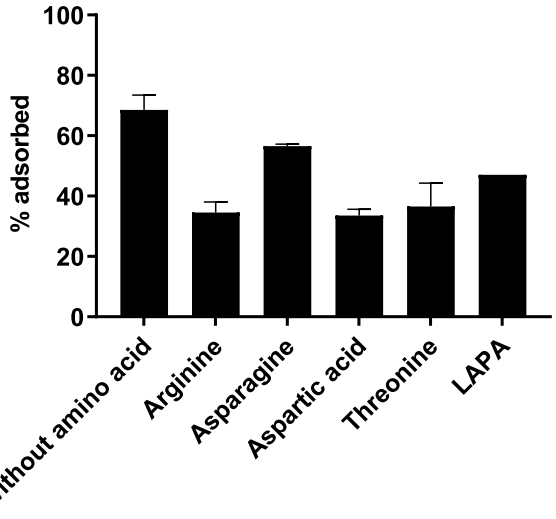


**Fig. 5. Influence of amino acids on the adsorption of lysozyme to aluminium phosphate.** Sonicated aluminium phosphate containing 0.85 mg/mL $Al^{3+}$ ions was mixed with 50 mM amino acid and 2.1 mg/mL fluorescent-labelled lysozyme. Samples were incubated for one hour at room temperature and centrifuged at 16,000*g*. The adsorption of lysozyme to aluminium phosphate was determined by subtracting the amount of free lysozyme in the supernatant from the amount of lysozyme that was added. Data is presented as mean ± range (n = 2).

plain aluminium phosphate nanoparticles.

In order to assess the immunogenicity of diphtheria toxoid adjuvanted with stabilised aluminium phosphate nanoparticles, mice were immunised on day 0 and 21. On day 35, mice were bled and their sera were analysed for total anti-diphtheria toxoid IgG titres and diphtheria toxin-neutralising antibodies. IgG titres of mice immunised with vaccines containing aluminium phosphate nanoparticles were significantly increased by the addition of arginine. On average, small changes in the diphtheria toxin-neutralising titres were detected, but none of them was significantly different from those elicited by the aluminium phosphate nanoparticles without amino acid (Fig. 7A and B).

## 4. Discussion

Aluminium salts are the major adjuvants applied in human vaccines. Commonly used aluminium-containing adjuvants aggregate in water. The adjuvant effect may be affected by the physicochemical properties of the particles. For example, small particles may induce less local irritation compared to big particles. In addition, an increased surface area, which can be obtained by decreasing particle size, may be related to an increased adsorption capacity of antigen to aluminium salts. In this regard, a smaller amount of nanosized adjuvant is needed to adsorb an equal amount of antigen compared to microsized adjuvant, reducing the side effects of aluminium salts. In this study, we prepared nanoparticles by sonication of commercially available aluminium phosphate. The nanoparticles showed long-term aggregation, which could be partially prevented by addition of particular amino acids. Arginine, asparagine, aspartic acid, LAPA and threonine were selected to study their stabilisation effects more extensively. Arginine and threonine were selected as controls, because arginine induced aggregation of aluminium phosphate nanoparticles to micro particles while the aggregation was minimal in the presence of threonine. Asparagine and aspartic acid were chosen to investigate the effect of substitution of the amide group with a carboxyl group. LAPA includes a phosphate group that can exchange with the hydroxyl and phosphate groups on aluminium phosphate, the so called ligand exchange. Together, this selection may help to shed light on the mechanism of stabilisation of aluminium phosphate nanoparticles.

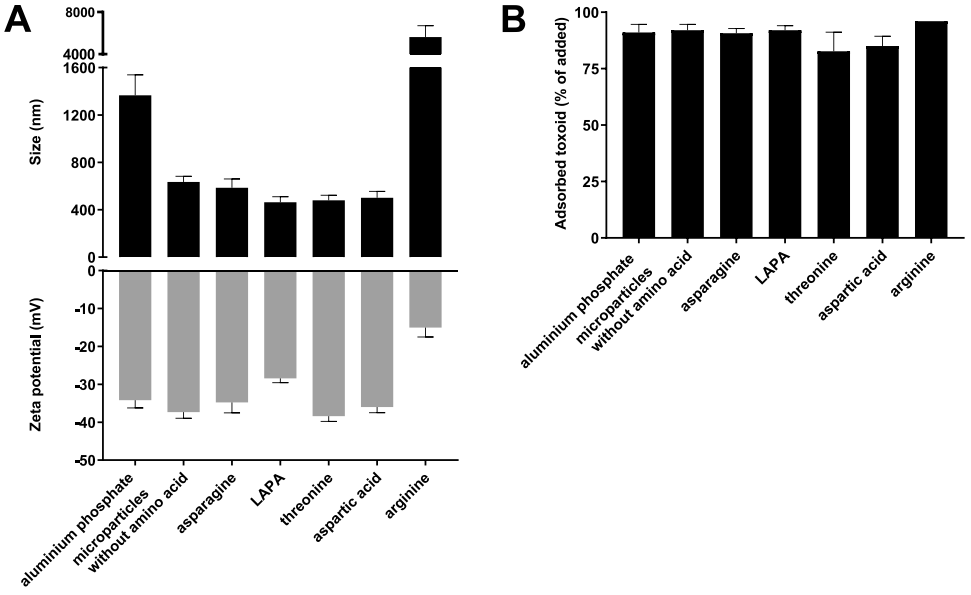


**Fig. 6. Size (A), zeta potential (A) and adsorption degree (B) of vaccines.** The adsorption degree was measured by centrifugation of the vaccines and determination of diphtheria toxoid in the supernatants. Data is presented as % adsorbed diphtheria toxoid with 100% equals the added amount diphtheria toxoid. Data is presented as mean ± SD (n = 3).

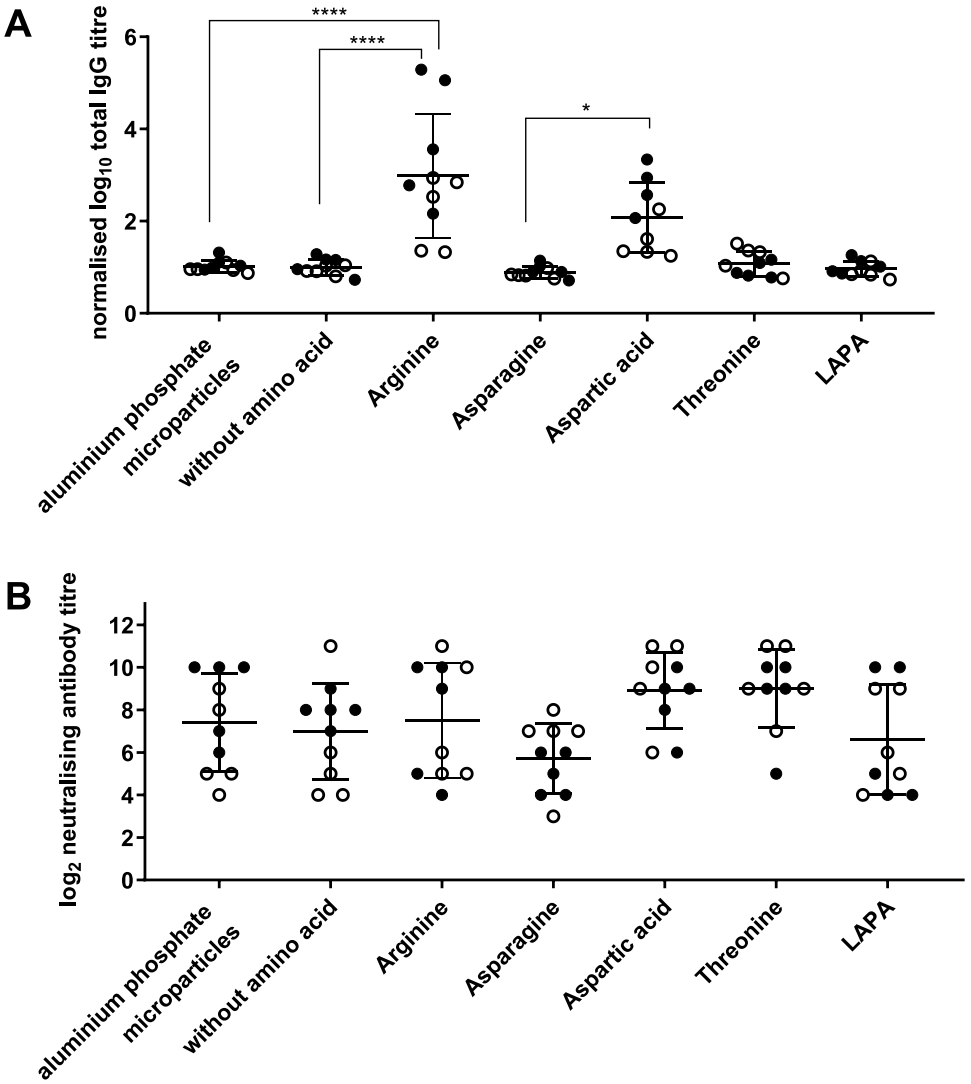


**Fig. 7. Total anti-diphtheria IgG titres (A) and neutralising antibodies (B) of sonicated aluminium phosphate in absence of presence of amino acids.** 8-week old BALB/c mice (five female and five male mice, open and closed symbols respectively per group) were immunised s.c. with 500 µL containing 0.85 mg $Al^{3+}$, 50 mM amino acid and 1.5 Lf diphtheria toxoid on day 0 and day 21. Mice were bled on day 35 and sera were analysed for total anti-diphtheria IgG and neutralising antibodies. Data is expressed as $\log_{10}$ of the serum dilution giving 50% of the maximum optical density at 450 nm normalised to the average titre of mice immunised with plain aluminium phosphate nanoparticles (A) or as $\log_2$ of the first serum dilution giving 80% of the maximum optical density at 570 nm for each individual curve (B). P-values were determined by one-way ANOVA with Tukey's multiple comparison test (* = $p < 0.05$, **** = $p < 0.0001$).

In this study, the particle size of the aluminium phosphate salts was monitored by using DLS. Although this is a convenient screening tool to estimate the particle size in the nanometre size range, DLS is not very accurate for polydisperse samples and may miss large micrometre-sized aggregates of aluminium phosphate salts. Other techniques such as flow imaging microscopy or nanoparticle tracking analysis may therefore add relevant information about the particle size and its distribution [21,22].

Stabilisation of colloids can be achieved through 1) electrostatic stabilisation by formation of an electrical double layer around colloids, 2) steric stabilisation by adsorption of molecules to colloids, or 3) depletion stabilisation by free molecules in the dispersion medium. From the selected amino acids, arginine showed the most pronounced effects. The charge of arginine (pI 10.76) is opposite to that of aluminium phosphate nanoparticles (PZC 4.5) at pH 7.4. The decreased absolute zeta potential indicates that arginine forms a shield around aluminium phosphate nanoparticles, which is likely based on electrostatic interactions. Although this sometimes leads to electrostatic stabilisation, arginine induced aggregation instead of stabilisation. This may be induced by the formation of bridges between the positively charged arginine and the negatively charged aluminium phosphate nanoparticles. Indeed, the guanidinium groups of arginine and phosphate groups form salt bridges based on their electrostatic charge, leading to an almost covalent-like stability [23].

We investigated the interactions between amino acids and aluminium phosphate nanoparticles by analysis of the adsorption of amino acids to aluminium phosphate. Although LAPA contained phosphate groups that could contribute to ligand exchange with aluminium phosphate, this did not enhance adsorption of this compound compared to other amino acids. Amino acids are amphiprotic molecules and the investigated amino acids have both positively charged amine groups and negatively charged carboxyl groups. Thus, it is possible that the adsorption of the amino acids to aluminium phosphate nanoparticles is based on electrostatic interactions. In addition, the amino acids may be trapped within the porous structure of aluminium phosphate during the de-aggregation and re-aggregation of aluminium salts [24,25]. The adsorption of arginine was remarkably reduced compared to the other amino acids. This may be due to the formation of salt bridges between arginine and aluminium phosphate nanoparticles, preventing the formed micro particles from de-aggregation so that pores in which the amino acid can be trapped are not exposed.

Although the extent of protein adsorption was not influenced by sonication, the particle size might influence the immune response. For example, the mechanism of uptake is different for micro particles compared to nanoparticles. Li et al. showed that aluminium hydroxide nanoparticles showed a stronger antigen-specific vaccine adjuvant activity compared to aluminium hydroxide nanoparticles in vivo [16]. However, in this study there was no effect of sonication of aluminium phosphate on the adaptive immune response against diphtheria toxoid as shown by total anti-diphtheria IgG titres and toxin-neutralising antibody titres. This may be due to the local environment at the injection site, where salts that are present in body fluid may induce aggregation of the nanoparticles. In addition, biomolecules that are present in biological fluids may interact with the nanoparticles, forming a protein corona. The formation of a protein corona depends on the charge and stability of the colloidal particle [26,27]. Because the presence of amino acids altered the zeta potential of aluminium phosphate nanoparticles (Fig. 3), it is likely that the protein corona was also affected. This may have influenced the immune response in vivo.

The uptake of antigen by APCs is enhanced by poly-L-arginine after s.c. injection [28]. Although we did not use poly-L-arginine in our study, the presence of arginine in the formulation increased the total anti-diphtheria toxoid IgG titres significantly compared to plain aluminium phosphate nanoparticles, Nevertheless, the titres in this study were also more heterogeneous, which is undesirable. This is possibly related to the aggregation of aluminium phosphate nanoparticles in the presence of arginine, which caused a more heterogeneous size distribution. On the contrary, diphtheria-neutralising antibody titres did not increase in the presence of arginine. An increased total IgG titre is thus in this case not related to an improved functional immune response.

The current study demonstrates the effective size reduction of aluminium phosphate by sonication. While the obtained aluminium phosphate nanoparticles aggregated, long-term aggregation was effectively prevented by addition of threonine, asparagine, aspartic acid or LAPA. Sonication and the addition of amino acids did not affect the adaptive immune response induced by aluminium phosphate nanoparticles in combination with diphtheria toxoid, except for arginine which increased total IgG titres but not diphtheria-neutralising antibodies. By applying sonication to the aluminium phosphate micro particles and stabilising the obtained aluminium phosphate nanoparticles, a functional vaccine adjuvant with altered physicochemical properties was obtained. Coating of the nanoparticles with functional groups, such as amino acids, will shed light on the mechanism of action of the adjuvant and may reveal options to improve the current adjuvant. This may ultimately help to develop a new generation aluminium salt-based adjuvants with improved performance compared to the currently used aluminium-containing adjuvants.

## Acknowledgements

This project was funded by the Ministry of Health, Welfare and Sport, the Netherlands.

## Appendix A. Supplementary data

Supplementary material related to this article can be found, in the online version, at doi:https://doi.org/10.1016/j.colsurfb.2019.06.024.

## References

[1] A.T. Glenny, C.G. Pope, H. Waddingtom, H. Wallace, Immunological Notes XVII-XXIV, Immunological Notes, XVII, (1926).
[2] W.T.H. Harrison, Some observations on the use of alum precipitated diphtheria toxoid, Am. J. Public Health (1935).
[3] L.S. Burrell, C.T. Johnston, D.G. Schulze, J. Klein, J.L. White, S.L. Hem, Aluminium phosphate adjuvants prepared by precipitation at constant pH, Part II - physico-chemical properties, Vaccine 19 (2001) 6.
[4] J.D. Hem, C.E. Roberson, Form and stability of aluminium hydroxide complexes in dilute solution, Geological Survey Water-supply Paper 1827-A, (1967), p. 60.
[5] S. Iyer, H. Hogenesch, S.L. Hem, Relationship between the degree of antigen adsorption to aluminium hydroxide adjuvant in interstitial fluid and antibody production, Vaccine 21 (2003) 5.
[6] T.R. Ghimire, The mechanisms of action of vaccines containing aluminium adjuvants: an in vitro vs in vivo paradigm, Springerplus 4 (2015) 181.
[7] N.J. Temperton, D.C. Quenelle, K.M. Lawson, J.N. Zuckerman, E.R. Kern, P.D. Griffiths, V.C. Emery, Enhancement of humoral immune responses to a human cytomegalovirus DNA vaccine: adjuvant effects of aluminium phosphate and CpG oligodeoxynucleotides, J. Med. Virol. 70 (2003) 86–90.
[8] M. Huang, W. Wang, Factors affecting alum-protein interactions, Int. J. Pharm. 466 (2014) 139–146.
[9] L.S. Jones, L.J. Peek, J. Power, A. Markham, B. Yazzie, C.R. Middaugh, Effects of adsorption to aluminium salt adjuvants on the structure and stability of model protein antigens, J. Biol. Chem. 280 (2005) 13406–13414.
[10] H. Hogenesch, Mechanism of immunopotentiation and safety of aluminium adjuvants, Front. Immunol. 3 (2012) 406.
[11] B. Hansen, A. Sokolovska, H. HogenEsch, S.L. Hem, Relationship between the strength of antigen adsorption to an aluminium-containing adjuvant and the immune response, Vaccine 25 (2007) 6618–6624.
[12] T.R. Ghimire, R.A. Benson, P. Garside, J.M. Brewer, Alum increases antigen uptake, reduces antigen degradation and sustains antigen presentation by DCs in vitro, Immunol. Lett. 147 (2012) 55–62.
[13] S.J. Seeber, J.L. White, S.L. Hem, Predicting the adsorption of proteins by aluminium-containing adjuvants, Vaccine 9 (1991) 3.
[14] G.L. Morefield, A. Sokolovska, D. Jiang, H. HogenEsch, J.P. Robinson, S.L. Hem, Role of aluminium-containing adjuvants in antigen internalization by dendritic cells in vitro, Vaccine 23 (2005) 1588–1595.
[15] D.A. Kuhn, D. Vanhecke, B. Michen, F. Blank, P. Gehr, A. Petri-Fink, B. Rothen-Rutishauser, Different endocytotic uptake mechanisms for nanoparticles in epithelial cells and macrophages, Beilstein J. Nanotechnol. 5 (2014) 1625–1636.
[16] X. Li, A.M. Aldayel, Z. Cui, Aluminium hydroxide nanoparticles show a stronger

vaccine adjuvant activity than traditional aluminium hydroxide microparticles, J. Control. Release 173 (2014) 148–157.
[17] K. Muthurania, A.A. Ignatius, Z. Jin, J. Williams, S. Ohtake, Investigation of the sedimentation behavior of aluminium phosphate: influence of pH, ionic strength, and model antigens, J. Pharm. Sci. 104 (2015) 3770–3781.
[18] J.F. Art, A. Vander Straeten, C.C. Dupont-Gillain, NaCl strongly modifies the physicochemical properties of aluminium hydroxide vaccine adjuvants, Int. J. Pharm. 517 (2017) 226–233.
[19] H. Moayedi, B.B.K. Huat, S. Kazemian, T.A. Mohammad, Effect of stabilizer reagents on zeta potential of kaolinite and its relevance to electrokinetic treatment, J. Dispers. Sci. Technol. 33 (2012) 103–110.
[20] A.S. Woods, S. Ferre, Amazing stability of the arginine-phosphate electrostatic interaction, J. Proteome Res. 4 (2005) 6.
[21] S. Zolls, D. Weinbuch, M. Wiggenhorn, G. Winter, W. Friess, W. Jiskoot, A. Hawe, Flow imaging microscopy for protein particle analysis–a comparative evaluation of four different analytical instruments, AAPS J. 15 (2013) 1200–1211.
[22] V. Filipe, A. Hawe, W. Jiskoot, Critical evaluation of Nanoparticle tracking Analysis (NTA) by NanoSight for the measurement of nanoparticles and protein aggregates, Pharm. Res. 27 (2010) 796–810.
[23] A.S. Woods, S. Ferre, Amazing stability of the arginine-phosphate electrostatic interaction, J. Proteome Res. 4 (2005) 1397–1402.
[24] I.Z. Romero Mendez, Y. Shi, H. HogenEsch, S.L. Hem, potentiation of the immune response to non-adsorbed antigens by aluminium-containing adjuvants, Vaccine 25 (2007) 825–833.
[25] G.L. Morefield, H. HogenEsch, J.P. Robinson, S.L. Hem, Distribution of adsorbed antigen in mono-valent and combination vaccines, Vaccine 22 (2004) 1973–1984.
[26] R. Huang, R.P. Carney, F. Stellacci, B.L.T. Lau, Protein–nanoparticle interactions: the effects of surface compositional and structural heterogeneity are scale dependent, Nanoscale 5 (2013) 6928–6935.
[27] M. Lundqvist, J. Stigler, G. Elia, I. Lynch, T. Cedervall, K.A. Dawson, Nanoparticle size and surface properties determine the protein corona with possble implications for biological impacts, PNAS 105 (2008) 6.
[28] F. Mattner, J.-K. Fleitmann, K. Lingnau, W. Schmidt, A. Egyed, J. Fritz, W. Zauner, B. Wittmann, I. Gorny, M. Berger, H. Kirlappos, A. Otava, M.L. Birnstiel, M. Buschle, Vaccination with poly-L-arginine as immunostimulant for peptide vaccines: nduction of potent and long-lasting T-cell responses against cancer antigens, Cancer Res. 62 (2002) 5.